2011 American Control Conference
on O'Farrell Street, San Francisco, CA, USA
June 29 - July 01, 2011

Fuel-Assisted In-Cylinder Oxygen Fraction Transient Trajectory Shaping Control for Diesel Engine Combustion Mode Switching

Fengjun Yan and Junmin Wang*
Department of Mechanical and Aerospace Engineering
The Ohio State University

Abstract— **This paper presents a method for shaping the transient trajectory of in-cylinder oxygen fraction at intake valve closing (IVC) when combustion mode is switched from one to another in Diesel engines. To achieve this purpose, based on a non-equilibrium transient trajectory shaping (NETTS) control method, the fuel injection amount was adjusted within a given range (accommodated by adjusting fuel injection timing accordingly). Through air-path and fuel-path cooperative control, the transient trajectory of in-cylinder oxygen fraction can be bounded by a series of shaped-boundaries during tracking error converging. The dwell time between two consecutive combustion mode switching events can be effectively reduced. To evaluate the control algorithm, co-simulations were conducted using a GT-Power (a high-fidelity industry standard 1-D computational engine model software package) engine model and Matlab/SIMULINK.**

I. Introduction

Of late, advanced combustion modes, including homogenous charge compression ignition (HCCI), low temperature diffusion combustion (LTDC), and premixed charge compression ignition (PCCI), have been widely regarded as important combustion alternatives for the future internal combustion engines primarily due to their promising high fuel efficiencies and very low engine-out emissions [1][2][3][7][9][10][11]. During advanced multi-mode combustion engine transient operations, the desired engine in-cylinder conditions (ICCs), such as in-cylinder gas temperature, gas amount, and oxygen fraction, often instantaneously jump during combustion mode switching to avoid undesirable intermediate combustion events [1][13][14][16]. In the non-equilibrium period, the shapes of ICC trajectories after the (frequent) controller switching significantly affect the combustion events, so as to the engine fuel efficiency, emissions, drivability, and combustion noise. Therefore, it is necessary to ensure that the transient trajectories of ICC tracking errors travel through certain regions in the in-cylinder condition state-space during the combustion mode transitions.

Under this requirement, in comparison to air-path loop control, fuel-path loop control provides the possibility in dealing with the rapid transient operation control when combustion mode is switched from one to another. Particularly, unlike air-path control, in direct injection (DI) engines, the fueling parameter control is almost instantaneous and precise (except injection pressure which, however, does not affect the combustion if its variations are small). The fuel can be delivered to the combustion chamber precisely as desired in a given combustion cycle [20]. It has been demonstrated, by adjusting fuel injection timing accordingly, the engine indicated mean effective pressure (IMEP) can be maintained at the same level even with different fuel injection amounts [5]. Therefore, for transient operation control, a range for fuel injection amount adjustment exists without necessarily affecting the engine drivability. Even though changing injection timing may influence engine-out emissions to some extent, however, during such a short combustion mode transition period, emission becomes trivial comparing to the smoothness and stability of the combustion and engine operations. Thus, the authority of fuel-assisted control exists in handling the ICC transient trajectory shaping problem within a certain range.

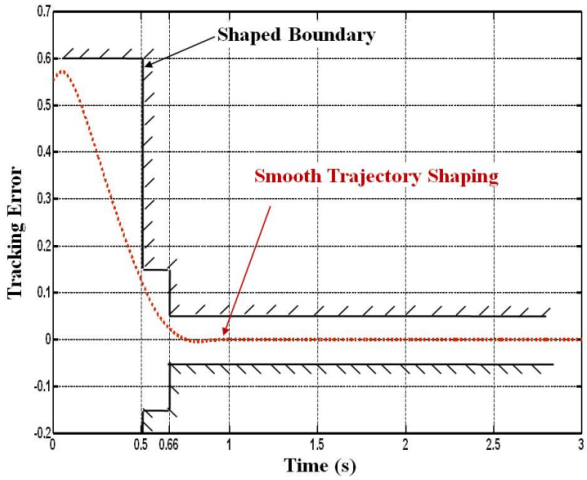

Fig. 1 A Typical Numerical Example for NETTS Control Algorithm [18].

To deal with such a NETTS control problem by the authority of fuel injection, we use a novel smooth transient trajectory shaping control method. As illustrated in Fig. 1, the objective of this method is to prevent the tracking error transient trajectory from violating the shaped-boundaries with input constraint consideration [18]. Such a control method is derived based on Barrier Lyapunov Functions (BLFs) [8][6] and backstepping techniques. The BLF candidate is a kind of positive definite function with a logarithmic form. A typical BLF candidate is as follows:

$$\bar{V} = \frac{1}{2} log \frac{k_b^2}{k_b^2 - z_1^2} + M, \quad (1)$$

where k_b is a positive constant called barrier parameter, z_1 is one of the arguments of the system to be bounded / shaped (typically it's the tracking error), M is a positive definite function with respect to the other arguments/states in the system. Provided that the initial condition of $|z_1|$ is smaller

*Corresponding author. Fengjun Yan (yan.373@osu.edu); Junmin Wang (wang.1381@osu.edu). This research was supported by National Science Foundation (NSF)-Control Systems Program Award CMMI-1029611.

than k_b, if we are able to find a control law, which can guarantee the derivative of $\bar{V}$ is negative definite, then $\bar{V}$ cannot go to infinite. From another aspect, $|z_1|$ cannot approach k_b. Otherwise, $\bar{V}$ will go to infinite, which is a contradiction. Motivated by such a BLF, smooth transient trajectory shaping method with input constraint concern was investigated in [19]. In this paper, in conjunction with the authority of rapid fuel-path control and the smooth transient trajectory shaping method, a fuel-assisted, in-cylinder oxygen fraction transient trajectory shaping control method is proposed.

The rest of this paper is organized as follows. The models of intake and exhaust manifolds and in-cylinder (at IVC) oxygen fractions are illustrated in section II. In section III, fuel-assisted in-cylinder oxygen fraction transient trajectory shaping method is proposed and described in details. To validate the proposed method, co-simulations between GT-Power (a high-fidelity industry standard 1-D engine computational model software) and Matlab/SIMULINK were conducted. Conclusive remarks are provided in section IV.

II. Oxygen Mass Fraction Models

In this section, the control-oriented models of oxygen fraction are described.

A. Manifold Oxygen Fraction Model

In [6], the models of air-path oxygen fractions were given as follows:

$$\dot{F}_e = \frac{RT_e}{P_e V_e}(F_{eo} - F_e), \tag{2}$$

$$\dot{F}_i = \frac{RT_i}{P_i V_i}[(F_a - F_i)W_a + (F_e - F_i)W_{egr}], \tag{3}$$

where F_e is the exhaust manifold oxygen fraction, F_i is the intake manifold oxygen fraction, W_a is the mass flow rate from ambience, and W_{egr} is the mass flow rate from EGR.

B. In-cylinder Oxygen Fraction Model

Fig. 2 shows the engine breathing and gas exchanging process for a cylinder. The control-oriented dynamic model of the in-cylinder gas oxygen fraction at IVC is derived as follows [17]. Based on the mass conservation, the following difference equations can be derived:

$$\begin{aligned} &m_c(k+1)F_c(k+1) \\ &= (m_c(k) + m_f(k))F_{eo}(k) + m_{ic}(k)F_i(k) + \\ &m_{ec}(k)F_e(k+1) - m_{ce}(k)F_{eo}(k), \end{aligned} \tag{4}$$

$$\begin{aligned} &m_e(k+1)F_e(k+1) = m_{ce}(k)\big(F_{eo}(k) - F_e(k)\big) + \\ &m_e(k)F_e(k), \end{aligned} \tag{5}$$

where k is the number of engine cycle.

With the assumption that the mass of inlet gas equals to that of outlet gas for both the cylinder and the exhaust manifold in each cycle [4][15], i.e.,

$$m_{ce}(k) = m_{ic}(k) + m_{ec}(k) + m_f(k), \tag{6}$$

we have

$$\begin{aligned} &m_c(k+1) = m_c(k) + m_f(k) + m_{ic}(k) + m_{ec}(k) - \\ &m_{ce}(k) = m_c(k), \end{aligned} \tag{7}$$

and also

$$m_e(k+1) = m_e(k). \tag{8}$$

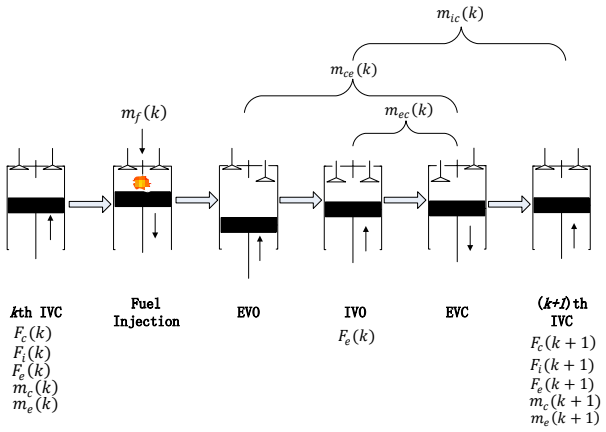

Fig. 2 Engine breathing and gas exchanging process from the *k*th IVC to (*k*+*1*)th IVC.

The oxygen fraction of the gas after combustion can be derived by:

$$\big(m_c(k) + m_f(k)\big)F_{eo}(k) = m_c(k)F_c(k) - m_f(k)\lambda_s, \tag{9}$$

i.e.

$$F_{eo}(k) = \frac{m_c(k)F_c(k) - m_f(k)\lambda_s}{m_c(k) + m_f(k)}, \tag{10}$$

where λ_s is the stoichiometric oxygen fuel mass ratio for complete combustion. Thus, the dynamic model of in-cylinder oxygen fraction was generated as:

$$\begin{aligned} F_c(k+1) &= \left(1 - \frac{m_{ce}}{m_c + m_f} + \frac{m_{ce}}{m_e}\cdot\frac{m_{ec}}{m_c + m_f}\right)F_c(k) + \\ &\frac{m_{ec}}{m_c}\cdot\left(1 - \frac{m_{ce}}{m_e}\right)F_e(k) + \frac{m_{ic}}{m_c}F_i(k) + \left(\frac{\lambda_s m_{ce}}{m_c(m_c + m_f)} - \right. \\ &\left.\frac{\lambda_s}{m_c} - \frac{m_{ec}}{m_c}\cdot\frac{m_{ce}}{m_e}\cdot\frac{\lambda_s}{m_c + m_f}\right)m_f(k). \end{aligned} \tag{11}$$

Here, we denote m_{ce}, m_{ec}, m_{ic}, m_c, m_e, m_f as $m_{ce}(k)$, $m_{ec}(k)$, $m_{ic}(k)$, $m_c(k)$ (or $m_c(k+1)$), $m_e(k)$ (or $m_e(k+1)$), $m_f(k)$ respectively for simplicity.

According to the discrete model above, the continuous mean-value models (MVM) can be easily derived as follows:

$$\begin{aligned} \dot{F}_c &= \left(-\frac{W_{ce}}{m_c + m_f} + \frac{120(W_e + W_f)}{Nm_e}\cdot\frac{W_{ec}}{m_c + m_f}\right)F_c + \\ &\frac{W_{ec}}{m_c}\left(1 - \frac{120(W_e + W_f)}{Nm_e}\right)F_e + \frac{W_{ic}}{m_c}F_i + \frac{\lambda_s W_{ce}}{m_c(m_c + m_f)} - \\ &\frac{N\lambda_s}{120(m_c + m_f)} - \frac{120W_{ec}}{Nm_c}\cdot\frac{W_{ce}}{m_e}\cdot\frac{\lambda_s}{m_c + m_f}m_f. \end{aligned} \tag{12}$$

In a typical control law design, the feedback EGR valve control signal depends on the value of oxygen fraction in the intake manifold. Here we denote W_{egr} a function of F_i, i.e. $W_{egr} = \varphi(F_i, t)$. Thus, (2), (3), and (12) can be written in a nonlinear strict feedback form as:

$$\begin{aligned} \dot{F}_c &= \left(-\frac{W_{ce}}{m_c + m_f} + \frac{120\big(W_e + W_f\big)}{Nm_e}\cdot\frac{W_{ec}}{m_c + m_f}\right)F_c \\ &+ \frac{W_{ec}}{m_c}\left(1 - \frac{120\big(W_e + W_f\big)}{Nm_e}\right)F_e \\ &+ \frac{W_e}{m_c}F_i \\ &+ \left[\frac{\lambda_s W_{ce}}{m_c\big(m_c + m_f\big)} - \frac{N\lambda_s}{120\big(m_c + m_f\big)}\right. \\ &\left. - \frac{120W_{ec}}{Nm_c}\cdot\frac{W_{ce}}{m_e}\cdot\frac{\lambda_s}{m_c + m_f}\right]m_f \\ &= f_1(F_c, t) + g_1 F_i, \end{aligned} \tag{13}$$

$$\dot{F}_i = \frac{RT_i}{P_iV_i}[(F_a - F_i)W_a + (F_e - F_i)W_{egr}] = \frac{RT_i}{P_iV_i}[(F_a - FiWa+(Fe-Fi)\varphi(Fi,t)]=f2Fi,t+g2Fe, \quad (14)$$

$$\dot{F}_e = \frac{RT_e}{P_eV_e}W_{ce}(F_{eo} - F_e) = -\frac{RT_e}{P_eV_e}W_{ce}F_e + \frac{RT_e}{P_eV_e}\frac{W_{ce}}{m_c+m_f}m_cF_c - \frac{RT_e}{P_eV_e}\frac{W_{ce}}{m_c+m_f}\lambda_s m_f = f_3(F_e,t) + g_3m_f. \quad (15)$$

In Diesel engines, due to the high compression ratios, the influence from trapped residual gas in cylinder to in-cylinder oxygen fraction at IVC is minor comparing the burnt gas from external EGR loops. With this consideration, F_c in (12) is assumed to be mainly influenced by F_i, so the term m_f and F_e in (13), which are related to the trapped residual gas and the gas from exhaust manifold during valve overlapping, are trivial. Here we assume them as time-varying parameters.

The density of in-cylinder charge at IVC is considered the same as the one in intake manifold [7][12]. By the ideal gas law, m_c and m_e can be approximated as below:

$$m_c = \frac{p_iV_{IVC}}{RT_i}, \quad (16)$$

$$m_e = \frac{p_eV_e}{RT_e}. \quad (17)$$

By using the speed-density equation, the mass flow rate into the engine, W_{ic}, can be calculated as

$$W_{ic} = \frac{N\eta_v p_iV_{IVC}}{120RT_i}. \quad (18)$$

Here, p_i, p_e and T_i, T_e are pressures and temperatures of intake manifold and exhaust manifold, respectively. η_v is the engine volumetric efficiency. R is the ideal gas constant.

The mass flow rate from cylinder to exhaust manifold, W_{ce}, can be illustrated as:

$$W_{ce} = W_e + W_f + W_{ec}, \quad (19)$$

where W_{ec} is the mass flow rate from exhaust manifold to cylinder during intake and exhaust valve overlapping, illustrated as:

$$W_{ec} = \frac{Nm_{ec}}{120}. \quad (20)$$

Here, the mass flow from exhaust manifold to cylinder during intake and exhaust valve overlapping period can be derived by using the model developed in [12]:

$$m_{ec} = (\Delta m_{restV} + \Delta m_{restB}), \quad (21)$$

where Δm_{restV} and Δm_{restB} are the mass flow caused by the volume change and pressure difference, respectively. The two terms can be written as:

$$\Delta m_{restV} = d_i \cdot q_1, \quad (22)$$

$$\Delta m_{restB} = SGN(p_e - p_i)A_K\sqrt{2dABS(p_e - p_i)} \cdot \frac{dt}{d\varphi}q_2, \quad (23)$$

where

$$q_1 = \int_{IVO}^{EVC}\frac{dV}{d\varphi}\cdot\frac{{\alpha_{K_{exh}}}^2}{{\alpha_{K_{exh}}}^2+{\alpha_{K_{int}}}^2}d\varphi, \quad (24)$$

$$q_2 = \int_{IVO}^{EVC}\frac{\alpha_{K\_exh}\cdot\alpha_{K\_int}}{\sqrt{{\alpha_{K\_exh}}^2+{\alpha_{K\_int}}^2}}d\varphi. \quad (25)$$

Here, d_i is the in-cylinder charge density during valve overlapping, and can be approximated by the intake manifold charge density calculated through the ideal gas law. $ABS(p_e - p_i)$ denotes the absolute value of pressure difference between intake manifold and exhaust manifold. A_K is the piston surface area. $\alpha_{K_{int}}$ and $\alpha_{K_{exh}}$ are piston surface area effective parameters. φ is the crank angle.

III. Fuel-Assisted In-Cylinder Oxygen Fraction NETTS control

A. Outline of Fuel-Assisted In-Cylinder Oxygen Fraction Transient Control

In typical transient of combustion mode switching, to satisfy the engine performance and safety, the in-cylinder conditions need to be changed in a quite small time interval and within a shaped-boundary. Here we define the desired (ideal) trajectory during switching as a jump.

Assume that, without affecting the IMEP performance, by adjusting the injection timing, the fuel injection amount has a tunable range, $[-\Delta m_f, +\Delta m_f]$. In the oxygen fraction reference switching, the initial value is $F_{c,0}$ and the objective value is $F_{c,d}$. Then, the control law can be designed in the following steps:

Step 1 (before trajectory shaping). Apply typical air-path control method and the maximal fuel adjustment towards the objective reference $F_{c,d}$, i.e., when $F_{c,d}$ is smaller than $F_{c,0}$, the fuel amount is $\bar{m}_f + \Delta m_f$, where $\bar{m}_f$ is the nominal fuel injection amount, and vice versa. In such a way, the oxygen fraction can decrease in its fastest rate.

Step 2 (trajectory shaping bound estimation). Based on the in-cylinder oxygen fraction model and smooth transient trajectory shaping method proposed later, a NETTS application range, ΔF_c around $F_{c,d}$, can be estimated with respect to Δm_f. Within this range, Δm_f is sufficient for the in-cylinder oxygen fraction smooth transient trajectory shaping.

Step 3 (trajectory shaping). When the F_c approaches the $F_{c,d} \pm \Delta F_c$, the smooth transient trajectory shaping control law is activated. Such a control law can guarantee the F_c travels within a shaped-boundary before it converges to $F_{c,d}$.

To be noted, in such a control method, the air-path loop control is also conducted simultaneously and the fuel-assisted control law is used to reduce the dwell time and guarantee the shape of the in-cylinder oxygen transient trajectory.

B. The Systems under Consideration

The main algorithm utilized here is to shape of the transient non-equilibrium tracking control error of nonlinear SISO strict feedback systems. F_i, F_c, F_e and m_f are denoted by x_1, x_2, x_3 and, u, respectively.

Thus, the mass of oxygen fraction models in (13), (14), and (15) can be written as:

$$\dot{x}_i = f_i(\bar{x}_i) + g_i(\bar{x}_i)x_{i+1}, i = 1,2, \quad (26)$$

$$\dot{x}_3 = f_3(\bar{x}_3) + g_3(\bar{x}_3)u, \quad (27)$$

with the system output being

$$y = x_1. \quad (28)$$

Denote y_d the desired reference and $z_1 = x_1 - y_d$ the tracking error. $\bar{x}_i$ represents the state vector $[x_1, \dots, x_i]$. The following assumptions are made: 1) $y_d, \dot{y}_d, y_d^{(2)}, y_d^{(3)}$ are bounded. 2) f_i,g_i are smooth functions and themselves and

their derivatives have known bounds in the definitional domain. 3) There exists a constant g_0 such that:

$$|g_i| \geq g_0 > 0. \tag{29}$$

C. Smooth Transient Trajectory Shaping Method

In step 2 and step 3, the smooth trajectory shaping method (STS) with control signal constraint [18][19] is used. In this subsection, the application of STS with respect to the system (26)-(28) is described.

Before we introduce the smooth trajectory shaping method, a single Barrier Lyapunov Function (SBLF) method is presented. By this method, the trajectory tracking error can be guaranteed within a single constant bound. Then, by Theorem 1, the trajectory shaping method will be proposed with respect to a series of shaped-boundaries. Based on the system in subsection III-B, SBLF method can be generated by the following steps:

Step 1: choose the candidate Barrier Lyapunov Function as:

$$V_1 = \frac{1}{2} log \frac{k_{b1}^2}{k_{b1}^2 - z_1^2}. \tag{30}$$

Note whereas $|z_1|$ approaches to k_{b1}, this Barrier Lyapunov Function will approach to infinity. Provided the Lyapunov Function cannot be greater than its initial value V_0, $|z_1|$ should be bounded by k_{b1}. To satisfy such a condition, the derivative of the Barrier Lyapunov Function (BLF) is proved to be negative definite by the backstepping techniques.

Take time derivative of V_1:

$$\dot{V}_1 = \frac{z_1 \dot{z}_1}{k_{b1}^2 - z_1^2} = \frac{z_1(f_1 + g_1(z_2 + \alpha_1) - \dot{y}_d)}{k_{b1}^2 - z_1^2}. \tag{31}$$

where the stabilizing function α_1 is chosen as:

$$\alpha_1 = \frac{1}{g_1}(-f_1 - k_1 z_1 + \dot{y}_d). \tag{32}$$

and z_{i+1} is defined as

$$z_{i+1} = x_{i+1} - \alpha_i, i = 1,2. \tag{33}$$

Then (31) can be written as:

$$\dot{V}_1 = -\frac{k_1 z_1^2}{k_{b1}^2 - z_1^2} + \frac{g_1 z_1 z_2}{k_{b1}^2 - z_1^2}. \tag{34}$$

By splitting the first term and completion of the square, (34) can be written as:

$$\dot{V}_1 = -\frac{k_1 z_1^2}{2(k_{b1}^2 - z_1^2)} - \frac{k_1(z_1 - g_1 z_2/k_1)^2}{2(k_{b1}^2 - z_1^2)} + \frac{g_1^2 z_2^2}{2k_1(k_{b1}^2 - z_1^2)} \leq N_1(z_1) - \frac{k_1 z_1^2}{4(k_{b1}^2 - z_1^2)} + \frac{g_1^2 z_2^2}{2k_1(k_{b1}^2 - z_1^2)}, \tag{35}$$

where $N_1(z_1) = -\frac{k_1 z_1^2}{4(k_{b1}^2 - z_1^2)}$ is negative definite with respect to z_1, for $|z_1| < k_{b1}$.

Step 2: Augment V_1 as:

$$V_2 = \frac{1}{2} log \frac{k_{b1}^2}{k_{b1}^2 - z_1^2} + \frac{1}{2} log \frac{k_{b2}^2}{k_{b2}^2 - z_2^2}, \tag{36}$$

where k_{b2} is chosen to be larger than $|z_2(0)|$.

The derivative of V_2 can be derived as:

$$\dot{V}_2 = N_1(z_1) - \frac{k_1 z_1^2}{4(k_{b1}^2 - z_1^2)} + \frac{g_1^2 z_2^2}{2k_1(k_{b1}^2 - z_1^2)} + \frac{z_2 \dot{z}_2}{k_{b2}^2 - z_2^2} = N_1(z_1) - \frac{k_1 z_1^2}{4(k_{b1}^2 - z_1^2)} + \frac{g_1^2 z_2^2}{2k_1(k_{b1}^2 - z_1^2)} + \frac{z_2(f_2 + g_2(z_3 + \alpha_2) - \dot{\alpha}_1)}{k_{b2}^2 - z_2^2}, \tag{37}$$

where z_3 is defined by (33). By choosing α_2 as:

$$\alpha_2 = \frac{1}{g_2}(-f_2 - k_2 z_2 + \dot{\alpha}_1). \tag{38}$$

(37) can be rewritten as:

$$\dot{V}_2 \leq N_1(z_1) - \frac{k_1 z_1^2}{4(k_{b1}^2 - z_1^2)} + \frac{g_1^2 z_2^2}{2k_1(k_{b1}^2 - z_1^2)} - \frac{k_2 z_2^2}{k_{b2}^2 - z_2^2} + \frac{g_2 z_2 z_3}{k_{b2}^2 - z_2^2} = N_1(z_1) + N_2(z_2) + W_1 + Y_1 - \frac{k_2 z_2^2}{4(k_{b2}^2 - z_2^2)}, \tag{39}$$

where

$$W_1 = -\frac{k_1 z_1^2}{4(k_{b1}^2 - z_1^2)} + \frac{g_1^2 z_2^2}{2k_1(k_{b1}^2 - z_1^2)} - \frac{k_2 z_2^2}{8(k_{b2}^2 - z_2^2)}. \tag{40}$$

$$Y_1 = -\frac{k_2 z_2^2}{2(k_{b2}^2 - z_2^2)} + \frac{g_2 z_2 z_3}{k_{b2}^2 - z_2^2}. \tag{41}$$

$N_2(z_2) = -\frac{k_2 z_2^2}{8(k_{b2}^2 - z_2^2)}$, which is negative definite with respect to z_2, for $|z_2| < k_{b2}$.

The following task is to manipulate W_1 negative by choosing proper k_1 and k_2. Let C be a constant such that $C \in (0, 1)$ and by choosing

$$k_1^2 > \frac{2g_1^2 k_{b2}^2}{(k_{b1} C)^2} + 2, \tag{42}$$

i.e.

$$k_1 > \frac{2g_1^2 k_{b2}^2}{k_1 (k_{b1} C)^2} + \frac{2}{k_1}. \tag{43}$$

Modify the first term of W_1 by substituting k_1 with the right side of (43). Then,

$$W_1 < -\frac{z_1^2}{2k_1(k_{b1}^2 - z_1^2)} - \frac{z_1^2 g_1^2 k_{b2}^2}{2k_1(k_{b1}C)^2(k_{b1}^2 - z_1^2)} + \frac{g_1^2 z_2^2}{2k_1(k_{b1}^2 - z_1^2)} - \frac{k_2 z_2^2}{8(k_{b2}^2 - z_2^2)}. \tag{44}$$

When $z_1^2 > (k_{b1} C)^2$, then the sum of the second and the third terms of W_1 in (44) is negative. Thus,

$$W_1 < -\frac{z_1^2}{2k_1(k_{b1}^2 - z_1^2)}. \tag{45}$$

When $z_1^2 < (k_{b1} C)^2$, then choose k_2 as:

$$k_2 > \frac{4g_1^2 k_{b2}^2}{k_1(k_{b1}^2 - (k_{b1} C)^2)}. \tag{46}$$

Submit the right side of (46) into k_2 of the last term of W_1. Then the last two terms of W_1 can be easily shown being negative. Consequently, W_1 satisfies (45) as well.

For Y_1, by completion of the square, we can get:

$$Y_1 = -\frac{k_2(z_2 - g_2 z_3/k_2)^2}{2(k_{b2}^2 - z_2^2)} + \frac{g_2^2 z_3^2}{2k_2(k_{b2}^2 - z_2^2)}. \tag{47}$$

By the manipulation above, the derivative of V_2 satisfies:

$$\dot{V}_2 \leq N_1(z_1) + N_2(z_2) - \frac{k_2 z_2^2}{4(k_{b2}^2 - z_2^2)} + \frac{g_2^2 z_3^2}{2k_2(k_{b2}^2 - z_2^2)}. \tag{48}$$

Step 3: Noting the last two terms of (35) and (48) are similar, we can use the same techniques by augmenting the Lyapunov Function by:

$$V_3 = \sum_{j=1}^{3} \frac{1}{2} log \frac{k_{bj}^2}{k_{bj}^2 - z_j^2}. \tag{49}$$

where k_{bj} is bigger than $|z_j(0)|$.

For the augmented V_3, similar procedure is conducted as above, and the stabilization functions are chosen as:

$$u = \frac{1}{g_3}(-f_3 - k_3 z_3 + \dot{\alpha}_2). \tag{50}$$

with k_3 satisfying:

$$k_3 > \frac{4g_2^2 k_{b3}^2}{k_2(k_{b2}^2 - (k_{b2} C)^2)}. \tag{51}$$

Then, the derivative of V_3 becomes:

$$\dot{V}_3 \leq \sum_{j=1}^{2} N_j(z_j) - \frac{k_3 z_3^2}{2(k_{b3}^2 - z_3^2)}. \tag{52}$$

As k_{bi} is chosen greater than $|z_i(0)|$, according to (49), when $|z_i|$ approaches to k_{bi}, V_3 will go to infinite. Here $i = 1,2,$ and 3. However, the conditions that the initial value of V_3 is finite and $\dot{V}_3$ is negative definite can ensure that V_3 must be finite. Thus, the control law here can guarantee $|z_i|$ stay within its respective bound k_{bi}. The final Lyapunov function V_3 is denoted as the overall Lyapunov function, i.e.:

$$V = V_3 = \sum_{i=1}^{3} \frac{1}{2} log \frac{k_{bi}^2}{k_{bi}^2 - z_i^2}. \quad (53)$$

In the overall Lyapunov function, for a clear interpretation, we use index i in k_{bi} and k_i instead of index j (which is only used in the augmentation proof process) in k_{bj} and k_j, to be consistent with the states z_i.

In the preceding SBLF algorithm, the tracking error can be bounded by a constant bound during converging. By using a series of Barrier Lyapunov Functions with a set of deceasing barrier parameters, the tracking error can be further shaped in transient period. Motivated by this, Theorem 1 was introduced in [18][19] for such a trajectory shaping purpose.

Theorem 1: Given a desired strictly decreasing boundary set: $K = \{k_{b1,1}, k_{b1,2}, \dots, k_{b1,m} | k_{b1,l} > k_{b1,l+1} > 0, l = 1, \dots, m-1\}$ and a buffer set $\Delta = \{\Delta_l | 0 < \Delta_l < k_{b1,l}, l = 1, \dots, m\}$, if the condition $|z_1(0)| \leq k_{b1,1} - \Delta_1 < k_{b1,1}$ is satisfied, then a series of control laws exists such that the tracking error has the following non-equilibrium trajectory-shaping property: Once z_1 enters the region $\{|z_1| \leq k_{b1,l} - \Delta_l\}$, $l = 1,2, \dots m$, it will be bounded by $k_{b1,l}$ until the equilibrium point is achieved. Here, the $k_{b1,l}$ and Δ_l ($k_{b1,l} > \Delta_l$) are the constant boundary and buffer size for the lth control law.

Proof. The proof of Theorem 1 is straightforward. Once the tracking error enter $\{|z_1| \leq k_{b1,l} - \Delta_l\}$, a new control law can be generated by the BLF as illustrated above, with respect to the new barrier parameter $k_{b1,l}$.

During control law switching transient, a smooth approximation is conducted as in (54), with which the control signal can be assured smooth by replacing $k_{i,l}$ with $\bar{k}_{i,l}(t)$.

$$\bar{k}_{i,l}(t) = k_{i,l} + \left(k_{i,l+1} - k_{i,l}\right) \left[\frac{1 - cos\left(\frac{\pi(t-t_l)}{a_l}\right)}{2}\right]^{n-1} > 0. \quad (54)$$

Here, a_l is the approximation duration.

As detailed in [18][19], by choosing the buffer condition properly (large enough), the stability and barrier conditions during transient and after switching can be guaranteed.

Remark 1: By (32), (33), (38), and (50), the bound of control signal can be estimated with respect to $k_{i,l}$, $k_{bi,l}$ and the bounds of f_i, g_i, and their derivatives in definitional domain. With such an estimation, given fuel adjustment range Δm_f, the in-cylinder oxygen fraction range ΔF_c can be determined, as mentioned in step 2 of subsection III-A.

IV. Simulation Studies

To show the effectiveness of the fuel-assisted control law, simulations through a high-fidelity, industry standard, 1D computational, GT-Power engine model were conducted. The speed of engine is constantly at 2500 rpm and the parameters used in the simulation are shown in Table 1. In the simulation, two in-cylinder oxygen fraction, F_c, trajectory switching methods were implemented separately. The first one is controlled only by the air-path mechanism for comparison purpose. For the air-path loop, a straightforward control law (feedforward control) was applied through a high pressure loop EGR flow rate control based on steady-state calibration. In the second case, besides the air-path control, fuel-assisted control was added to improve the transient performance. In this simulation, the reference of F_c jumped from 0.12 to 0.1.

TABLE I

Parameters in GT-Power Engine Model

Parameter	Value [a]
N	2500 rpm
R	286.9 J/kg/K
λ_v	3.329
V_i	4×10^{-4} m^3
V_e	4×10^{-4} m^3
V_{IVC}	0.782
k_b	0.01
k_1	2
k_2	13
k_3	34

Case 1: Air-path feedforward control. As shown in Fig. 3, the EGR valve was adjusted to the destination position once the reference jumped at 1 second. Due to the large time constant of the air-path loop, it took more than 2.5s for the transient process (we assume the tracking error converged if it is within 0.003).

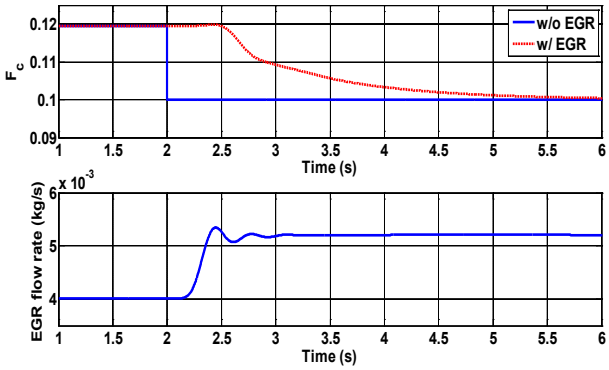

Fig. 3 Air-path feedforward control.

Case 2: Fuel-assisted air-path control. As shown in Fig. 4, the fuel injection amount was set to be the maximal adjustable value to reduce the dwell-time at the beginning of reference jumping. When the tracking error approaches a pre-designed range (0.11-0.1), the smooth transient trajectory shaping technique was applied.

By the comparisons with results in Fig. 5, the fuel-assisted transient trajectory shaping method can decrease the dwell time when the in-cylinder oxygen fraction reference jumped from one to another. The transient trajectory of the in-cylinder oxygen fraction can also be effectively shaped, which is valuable for combustion mode transition control.

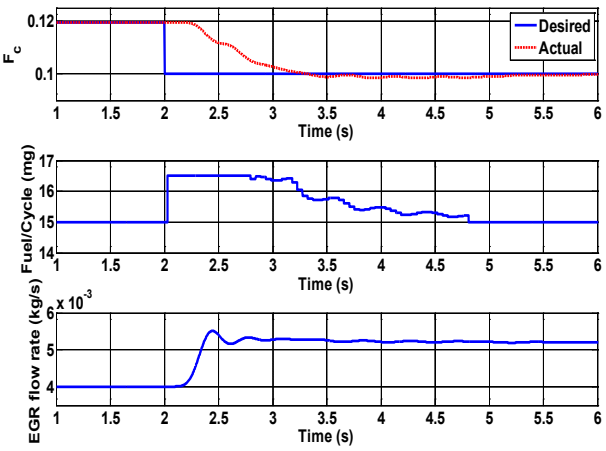

Fig. 4 Fuel-assisted air path control.

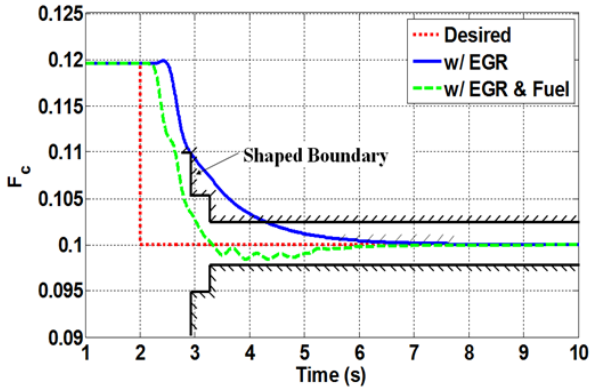

Fig. 5. Comparison between case 1 (without fuel-assisted control) and case 2 (with fuel-assisted control).

V. Conclusions and Future Work

In this paper, a fuel-assisted in-cylinder oxygen fraction trajectory shaping method based on the smooth non-equilibrium transient trajectory shaping control theory is proposed. Such a method can be implemented in control of multi-combustion mode engines. With simulation results, this method was shown to be effective. The dwell time during reference jump was largely shrunk and the transient trajectory could be guaranteed in a bounded region when tracking error converges to zero. Such transient control property certainties are beneficial for controlling the transient behaviors of advanced multi-mode combustion Diesel engines.

The future work will primarily include the experimental investigations of the methods for advanced combustion mode engine control.

References

[1] Akihama, K., Takatori, Y., Inaaki, K., Sasaki, S., and Dean, A., 2001, "Mechanism of the smokeless rich Diesel combustion by reducing temperature," SAE, Warrendale, PA. Tech. Rep. 2001-01-0655.

[2] Neely, G.D., Sasaki, S., Huang, Y., Leet, J.A. and Stewart, D.W., 2005, "New Diesel emission control strategy to meet US Tier 2 emissions regulations," SAE, Warrendale, PA, Tech. Rep. 2005-01-1091.

[3] Alriksson, M. and Denbratt, I., 2006, "Low temperature combustion in a heavy Diesel engine using high levels of EGR," SAE, Warrendale, PA, Tech. Rep. 2006-01-0075.

[4] Ammann, M., Fekete, N. P., Guzella, L., and Glattfelder, A. H., 2003, "Model-based control of the VGT and EGR in a turbocharged common-rail Diesel engine: theory and passenger car implementation," SAE Paper 2003-01-0357.

[5] Heywood, J. B., 1989, Internal Combustion Engine Fundamentals, McGraw Hill, New York.

[6] Tee, K.P., Ge, S.S. and Tay, E.H., 2009, "Barrier Lyapunov Functions for the Control of Output-Constrained Nonlinear Systems", Automatica, vol. 45, pp. 918-927.

[7] Killingsworth, N. J., Aceves, S. M., Flowers, D. L., and Krstic, M., 2006, "A simple HCCI engine model for control," Proceedings of the 2006 IEEE International Conference on Control Applications.

[8] Ngo, K.B., Mahony, R., and Jiang, Z.P., 2005, "Integrator Backstepping Using Barrier Functions for Systems with Multiple State Constraints," In Proc. 44th IEEE conf. Decision & control, pp. 8306-8312.

[9] Sasaki, S., Sarlashkar, J., Neely, G., Wang, J., Lu, Q., Sono, H., 2008, "Investigation of Alternative Combustion, Airflow Dominant Control and Aftertreatment Systems for Clean Diesel Vehicles," SAE Transactions-Journal of Fuels and Lubricants, Vol. 116, pp. 486 – 495.

[10] Sun, Y. and Reitz, R.D., 2008, "Adaptive Injection Strategies (AIS) for Ultra-Low Emissions Diesel Engines," SAE Paper 2008-01-0058.

[11] Thring, R.H., 1989, "Homogeneous-Charge Compression Ignition Engine," SAE Paper 892068.

[12] Koehler, U. and Bargende, M., 2004, "A Model for a Fast Prediction of the In-Cylinder Residual Gas Mass," SAE Paper, 2004-01-3053.

[13] Wang, J., 2008, "Hybrid Robust Air-Path Control for Diesel Engines Operating Conventional and Low Temperature Combustion Modes," IEEE Transactions on Control Systems Technology, Vol. 16, No. 6, pp. 1138 - 1151.

[14] Wang, J. and Chadwell, C., 2008. "On the Advanced Air-Path Control for Multiple and Alternative Combustion Mode Engines," SAE Paper 2008-01-1730.

[15] Wang, J., 2008, "Air fraction estimation for multiple combustion mode diesel engines with dual-loop EGR systems". Control Engineering Practice, Vol. 16, Issue 12, pp. 1479-1486.

[16] Wang, J., 2008, "Smooth In-Cylinder Lean-Rich Combustion Switching Control for Diesel Engine Exhaust-Treatment System Regenerations," SAE International Journal of Passenger Cars – Electronic and Electrical Systems, Vol. 1, No. 1, pp. 340 – 348.

[17] Fengjun Yan and Junmin Wang, "Design and Robustness Analysis of Discrete Observers for Diesel Engine In-Cylinder Oxygen Mass Fraction Cycle-by-Cycle Estimation," *IEEE Transactions on Control Systems Technology* (DOI: 10.1109/TCST.2010.2104151) (in press).

[18] Yan, F and Wang, J, 2010, "Non-Equilibrium Transient Trajectory Shaping Control via Multiple Barrier Lyapunov Functions for a Class of Nonlinear Systems," Proceedings of the 2010 American Control Conference, pp. 1695 - 1700, 2010.

[19] Yan, F. and Wang, J., 2010, "Input Constrained Non-Equilibrium Transient Trajectory Shaping Control for a Class of Nonlinear Systems," Proceedings of 49th IEEE Conference on Decision and Control, pp. 5156 - 5161, 2010.

[20] Fengjun Yan and Junmin Wang, "Common Rail Injection System Iterative Learning Control Based Parameter Calibration for Accurate Fuel Injection Quantity Control," *International Journal of Automotive Technology*, Vol. 12, No. 2, pp. 149 - 157, 2011.